Synchronization transition in networked chaotic oscillators: The viewpoint from partial synchronization

Chenbo Fu,[1,2,3] Weijie Lin,[2,3] Liang Huang,[4] and Xingang Wang[2,3,*]

[1]*Department of Automation, Zhejiang University of Technology, Hangzhou 310023, China*

[2]*School of Physics and Information Technology, Shaanxi Normal University, Xi'an 710062, China*

[3]*Department of Physics, Zhejiang University, Hangzhou 310027, China*

[4]*Institute of Computational Physics and Complex Systems, Lanzhou University, Lanzhou, Gansu 730000, China*

(Received 27 October 2013; published 12 May 2014)

Synchronization transition in networks of *nonlocally* coupled chaotic oscillators is investigated. It is found that in reaching the state of global synchronization the networks can stay in various states of partial synchronization. The stability of the partial synchronization states is analyzed by the method of eigenvalue analysis, in which the important roles of the network topological symmetry on synchronization transition are identified. Moreover, for networks possessing multiple topological symmetries, it is found that the synchronization transition can be divided into different stages, with each stage characterized by a unique synchronous pattern of the oscillators. Synchronization transitions in networks of nonsymmetric topology and nonidentical oscillators are also investigated, where the partial synchronization states, although unstable, are found to be still playing important roles in the transitions.

DOI: 10.1103/PhysRevE.89.052908 PACS number(s): 05.45.Xt, 89.75.Hc

I. INTRODUCTION

As a universal concept in nonlinear science, the synchronization of coupled nonlinear oscillators has attracted broad interest and has been extensively studied in fields such as physics, optics, chemistry, and biology [1–3]. In synchronization studies, a fundamental question is how the system dynamics is transited from the nonsynchronous to the synchronous states as a function of the system parameters, e.g., the coupling strength [4–9]. This question is not only crucial to the understanding of the synchronization mechanisms, but also has important implications to the operating and functioning of many realistic systems [2,3]. Previously, the studies of synchronization transition has been mainly focused on systems of small size and regular structures, where a number of interesting phenomena have been revealed. For two coupled chaotic oscillators, it has been shown that as the coupling strength increases, the oscillators could be first entrained in phase, i.e., the phase synchronization, and then entrained in amplitude, i.e., the complete synchronization [10]. For an ensemble of oscillators coupled through a regular structure, e.g., the coupled lattices or the globally coupled systems, it has been shown that in reaching the state of global synchronization, the oscillators could be synchronized into clusters, i.e., the partial (group) synchronization states [11–13]. In partial synchronization, oscillators inside a synchronous cluster are highly correlated, while they are loosely or not correlated if the oscillators belong to different clusters [14–23]. The specific form of the synchronous clusters, namely the synchronous pattern, depends not only on the dynamics of the oscillators, but also on the coupling function and coupling strength [24,25].

In the past decade, stimulated by the discoveries of the small-world and scale-free features in many natural and man-made systems [26,27], a new surge of research interest has been appeared in the study of oscillator synchronization, where the important roles of the network structure have been revealed and addressed [28–31]. It has been shown that, due to the reduced network average diameter, the synchronizability of small-world networks could be much higher than that of regular networks of the similar network parameters (e.g., the same network size and the same number of network links) [28,29], and, by adopting the weighted coupling schemes, the synchronizability of sale-free networks can be significantly improved and be higher than that of small-world or homogeneous random networks [30,31]. The existing studies, however, focus mainly on the two extreme cases of the network dynamics, namely the onset of synchronization and the state of global synchronization [32], while little attention has been paid to the intermediate states between the two extreme cases, i.e., the transition process of network synchronization. Different from the regular networks, where the synchronization transition is more dependent on the oscillator parameters (e.g., the parameter configuration) [33,34], in complex networks the transition is crucially dependent on the network topological structures, as has been well recognized in the recent studies [35–38]. In Ref. [35], the authors have studied the synchronization transition in heterogeneous networks and found that the transition process is largely affected by the degree distribution of the network nodes. In Ref. [36], the authors have compared the paths to global synchronization between the homogeneous and heterogeneous networks, where it is found that the transition scenario relies on the network heterogeneity. In Ref. [37], based on the dynamical properties of the synchronization transition, the authors have proposed a new method capable of identifying the topological scales and hierarchical structures in some realistic complex networks. Despite the progress made, the picture of synchronization transition in complex networks is still not very clear, and many questions remain open, say, for instance, how to characterize precisely the nonsynchronous states [38].

In the present work, from the viewpoint of partial synchronization, we revisit the problem of synchronization transition by network models beyond the regular structures. More

*Corresponding author: wangxg@snnu.edu.cn

specifically, we adopt networks possessing both the features of topological symmetry (like the regular networks) and nonlocal connections (like the complex networks) and investigate how the system is transited from the nonsynchronous to synchronous states as a function of the coupling strength. Different from the previous studies of synchronization transition, here more attention is paid to the identification of some *special states* in the nonsynchronous regime, and their roles in the synchronization transition are explored. Interestingly, we find that for the employed network models, the synchronization transition can be clearly divided into different stages, with each stage characterized by a specific pattern of synchronized oscillators, i.e., a partial synchronization state [16–19,21–23]. The form of the synchronous pattern is found to be closely dependent on the network topological symmetries, and, as the coupling strength increases, it could transit from one form to other forms in an intermittent fashion. The present work is stimulated by the study in Ref. [21], in which partial synchronization in networks of nonlocally coupled oscillators has been investigated, and a criterion has been given for the stability of the partial synchronization states.

The rest of the paper is organized as follows. In Sec. II, we present our model of networked oscillators and describe the phenomena obtained in numerical simulations, including the transition process and the partial synchronization states. In Sec. III, by a generalized method of eigenvalue analysis, we give an analysis on the stability of the partial synchronization states, where the crucial roles of the network topological symmetries on partial synchronization are addressed. In Sec. IV, we investigate the transition between different partial synchronous states, in which the phenomenon of on-off pattern intermittency are reported and studied. In Sec. V, we extend our study to the cases of asymmetric networks and nonidentical oscillators. In Sec. VI, we give our discussions and conclusion.

II. MODEL AND PHENOMENA

We consider the following model of networked chaotic oscillators [30,31],

$$\dot{\mathbf{x}}_i = \mathbf{F}(\mathbf{x}_i) - \varepsilon \sum_{j=1}^{N} c_{ij}[\mathbf{H}(\mathbf{x}_j) - \mathbf{H}(\mathbf{x}_i)], \qquad (1)$$

with $i, j = 1, \ldots, N$ the oscillator (node) indices and $\mathbf{x}$ the state variables. In the isolated form, the dynamics of each oscillator is governed by the equation $\dot{\mathbf{x}}_i = \mathbf{F}(\mathbf{x}_i)$, which, for the sake of simplicity, is set to be identical for the oscillators. The coupling relationship of the oscillators is described by the matrix $\mathbf{C}$, with $c_{ij} = -w_{ij}/\sum_j w_{ij}$. Here w_{ij} represents the weight of the link L_{ij} that connects nodes i and j in the network. By a uniform coupling strength ε, the connected oscillators influence each other through the function $\mathbf{H}(\mathbf{x})$. This model of linearly coupled oscillators has been widely adopted in the literature for synchronization studies, and many of its dynamical properties have been well explored [3]. In particular, the stability of the global synchronization state can be conveniently analyzed by the method of master stability function (MSF) [39–41], which shows that for the typical nonlinear oscillators, the synchronizability of a network is generally determined by the extreme eigenvalues of the network coupling matrix $\mathbf{C}$. The MSF method, however, applies only to the state of global network synchronization, which is not suitable for analyzing the nonsynchronous states [42].

We start by investigating the synchronization transition of a simple network possessing topological symmetries and containing nonlocal connections. The structure of the network model is presented in Fig. 1(a), which is constructed by a six-node ring lattice and three nonlocal connections (shortcuts). To capture the feature of weighted links widely observed in realistic networks [43], we set $w_{1,4} = 0.8$ for the link $L_{1,4}$ and $w = 1$ for the other links. This network model combines the features of both regular (the symmetric topology) and complex (the nonlocal connections) networks and is expected to present a hybrid synchronization behavior. Specifically, because of the symmetric topology (i.e., the reflection symmetries, $\mathbf{S}_1$ and $\mathbf{S}_2$, and the rotation symmetry, $\mathbf{S}_3$), the network is expected to generate the partial synchronization state, just like the case of regular networks [17,19]. In the meantime, due to the nonlocal connections, the network structure is heterogeneous; i.e., some nodes have more connections than others. As has been revealed in previous studies of complex network synchronization [35,36], this heterogeneity will make the network nodes behave very differently in the transition to synchronization, resulting in the complicated synchronization behaviors in the nonsynchronous regime.

In simulating, we adopt the chaotic Lorenz oscillator as the node dynamics, which in its isolated form is described by equations $(dx/dt, dy/dt, dz/dt)^T = [\alpha(y-x), rx - y - xz, xy - bz]^T$. By the parameters $\alpha = 10$, $r = 35$, and $b = 8/3$, the isolated oscillator is chaotic, with the largest Lyapunov exponent about 1.05 [44]. The coupling function is chosen as $\mathbf{H}([\mathbf{x},\mathbf{y},\mathbf{z}]^{\mathbf{T}}) = [0,x,0]^T$; i.e., the x variable is coupled to the y variable [41]. In Fig. 1(b), we plot the variation of the system synchronization error, $\delta = \langle \sum_i |x_i - \bar{x}|/N \rangle$, as a function of the coupling strength, ε. Here $\bar{x}(t) = \sum_i x_i(t)/N$ is the averaged x variable of the oscillators at the moment t, and $\langle \cdots \rangle$ represents the time average over a period of $T = 1 \times 10^3$. It is seen in this figure that, as ε increases from 0, the value of δ is gradually decreased, finally reaching 0 at $\varepsilon_c \approx 13.1$ (the state of global synchronization). This scenario of monotonic decrease of δ has been typically observed in the synchronization transition of coupled chaotic oscillators, including both the regular and the complex network structures [4,9]. However, in reaching to the state of global synchronization, we notice in Fig. 1(b) that in some regions of the parameter space the value of δ is quickly decreased, i.e., $\varepsilon \in (0,6.5)$ and $\varepsilon \in (10,\varepsilon_c)$, while in the region $\varepsilon \in [6.5,10]$ the decrease of δ is quite slow, exhibiting a remarkable flat. This leads to question in which we are interested and want to explore: *Why does the system synchronization error behave in such a manner?*

To explore the transition behaviors observed in Fig. 1(b), we go on to investigate the synchronization relationship among the individual nodes during the transition process. In doing this, we calculate the difference between x_i and x_2 (i.e., using the second node as the reference) and check how this difference varies with the coupling strength. Defining the difference as $\delta x_i = \langle |x_i - x_2| \rangle$, in Fig. 1(c) we plot the variation of δx_i as a function of ε. Interestingly, it is found that before the state of global synchronization, some of the oscillators have been already synchronized. More specifically,

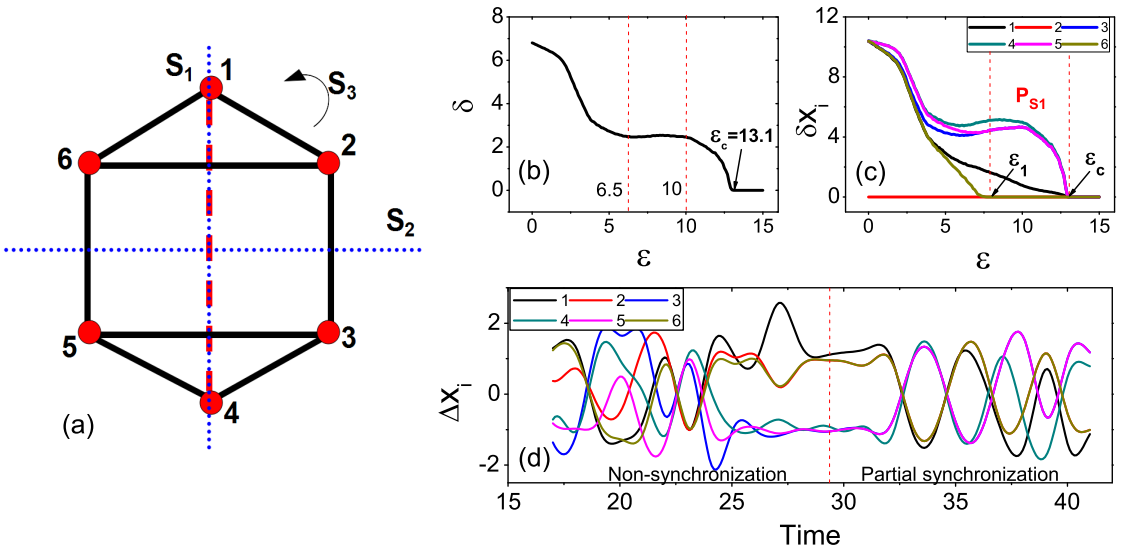

FIG. 1. (Color online) The synchronization transition of a six-node network model, with the dynamics of the isolated oscillator (node) being governed by the chaotic Lorenz oscillator. (a) The network structure. The weight of the link $L_{1,4}$ is 0.8, and it is 1 for the other links. The network structure possesses two reflection symmetries, $\mathbf{S}_1$ and $\mathbf{S}_2$, and one rotation symmetry, $\mathbf{S}_3$ (180° rotation). (b) The variation of the system synchronization error, $\delta = \langle \sum_i |x_i - \bar{x}|/N \rangle$, as a function of the coupling strength, ε. Global synchronization is achieved at about $\varepsilon_c = 13.1$. (c) The variation of the synchronization relationship of the oscillators, characterized by the node synchronization error $\delta x_i = \langle |x_i - x_2| \rangle$, as a function of ε. Partial synchronization represented by the symbol sequence $\mathbf{P}_{S1} = (a,b,c,d,c,b)$ is observed in the range $\varepsilon \in (\varepsilon_1, \varepsilon_c)$, with $\varepsilon_1 \approx 8.1$. (d) With $\varepsilon = 8.4$ and random initial conditions, the time evolution of the normalized synchronization errors Δx_i. It is seen that, after a transient time of about $t = 29$, the system reaches the partial synchronization state characterized by $\mathbf{P}_{S1}$.

in the region of $\varepsilon_1 = 8.1 < \varepsilon < \varepsilon_c$, the second oscillator is synchronized with the sixth oscillator, while the third oscillator is synchronized with the fifth oscillator. That is, in this region the system stays in a partial synchronization state. To have more details on the generation of this partial synchronization state, by $\varepsilon = 8.4$ and the random initial conditions, we plot in Fig. 1(d) the time evolution of the normalized synchronization errors of the oscillators, $\Delta x_i = (x_i - \bar{x})/\Delta x_{\text{ave}}$, with $\Delta x_{\text{ave}} = \sum_i |x_i - \bar{x}|/N$ the scaling factor. It is seen that, after a short transient period about $t = 29$, we have $\Delta x_2 = \Delta x_6$ and $\Delta x_3 = \Delta x_5$, indicating that the system has reached the above mentioned partial synchronization state. Here, to facilitate the analysis of partial synchronization, we characterize each partial synchronization state by a symbol sequence $\mathbf{P}$ [23]. Each symbol in the sequence represents a unique oscillator trajectory, and the symbols are ordered by the node indices. For instance, the state of partial synchronization shown in Fig. 1(d) is characterized by the sequence $\mathbf{P}_{S1} = (a,b,c,d,c,b)$. The subscript describes the symmetry that the symbol satisfies, which is explained in detail later. By the symbol sequence, we can readily figure out the number of synchronous clusters in the network (as the number of different symbols in the sequence), as well as the contents of each synchronous cluster (the nodes of the same symbol in the sequence).

By the critical couplings ε_1 and ε_c, the parameter space of ε can be divided into three regimes: nonsynchronization ($\varepsilon < \varepsilon_1$), partial synchronization ($\varepsilon_1 < \varepsilon < \varepsilon_c$), and global synchronization ($\varepsilon > \varepsilon_c$). With this division of the parameter space, the underlying mechanisms of the transition behavior shown in Fig. 1(b) can be understood: The fast decrease of the system synchronization error in the region of $\varepsilon \in (0,6.5)$ [$\varepsilon \in (10,\varepsilon_c)$] is due to the reaching of the partial (global) synchronization state. As depicted in Fig. 1(c), as ε approaches ε_1, the sixth oscillator is quickly synchronized to the second oscillator, while in this process the system synchronization error is also found to be quickly decreased [Fig. 1(b)]. This is also the case nearby the point of global synchronization. As shown in Fig. 1(c), as ε reaches ε_c, oscillators 3, 4, and 5 (the upper three curves) are quickly synchronized to the other three oscillators (the lower three curves), which in Fig. 1(b) corresponds to a fast decrease of the system synchronization error. Interestingly, in Fig. 1(c) it is also seen that in the region of $6.5 < \varepsilon < 10$, the synchronization errors of oscillators 3, 4, and 5 are not decreased with ε. This is solely a phenomenon induced by partial synchronization, as the increase of ε will also enhance the partial synchronization, which hinders the achievement of global synchronization [8]. As a result, the system synchronization error remains almost unchanged in this region.

Regarding the significant roles of partial synchronization played in the synchronization transition, a detailed analysis of the properties of the partial synchronization states therefore becomes necessary. For systems of networked oscillators, a question naturally arises: For the given network dynamics, can we figure out the partial synchronization states and estimate their stabilities, based only on the information of the network topology? In the following section, we address this question by the method of eigenvalue analysis.

III. STABILITY ANALYSIS OF PARTIAL SYNCHRONIZATION STATES

Whether or not a partial synchronization state can be generated in a network is closely related to the network

topological symmetries [45]. Take the network of Fig. 1(a) as an example. The network possesses three symmetries: two reflection symmetries, $\mathbf{S}_1$ and $\mathbf{S}_2$, and one rotation symmetry, $\mathbf{S}_3$ (which is a combination of $\mathbf{S}_1$ and $\mathbf{S}_2$). For each topological symmetry, if we set artificially the initial states of the oscillators to be satisfying the same symmetry as the network topology, i.e., the system is started from a specific pattern of initial conditions, then during the process of system evolution this pattern is maintained. For instance, if we set the initial conditions of the paired nodes, (2,6) and (3,5), to be identical (according to the reflection symmetry $\mathbf{S}_1$), then as time increases the system will stay in the partial synchronization state characterized by the sequence $\mathbf{P}_{S1} = (a,b,c,d,c,b)$. This is simply because the paired nodes are surrounded by the same set of neighbors and are influenced by the same signal sequence.

While each topological symmetry is supportive to a specific state of partial synchronization, not all these states are observable in the synchronization transition. That is, some of the states are unstable. This is evidenced in Fig. 1(c), where during the process of synchronization transition only the state supported by the symmetry $\mathbf{S}_1$ is observed, while the other two states, supported by symmetries $\mathbf{S}_2$ and $\mathbf{S}_3$, do not appear. The stability of the partial synchronization states can be analyzed by the method of eigenvalue analysis, with the details as follows. (This method is originated from the method of eigenvalue analysis proposed in Ref. [21], but is generalized to any network symmetry here.) Let $\mathbf{x}_s$ be the synchronous manifold of the system (the manifold for global synchronization) and $\delta\mathbf{x}_i = \mathbf{x}_i - \mathbf{x}_s$ be the infinitesimal perturbations added to the oscillator trajectories; then in the linearized form the perturbations will evolve according to

$$\delta\dot{\mathbf{x}}_i = \mathbf{DF}(\mathbf{x}_s) - \varepsilon \sum_{j=1}^{N} c_{ij}\mathbf{DH}(\mathbf{x}_s)(\delta\mathbf{x}_j - \delta\mathbf{x}_i), \tag{2}$$

where $\mathbf{DF}$ and $\mathbf{DH}$ are the Jacobian matrices of the corresponding vector functions evaluated on $\mathbf{x}_s$. Projecting $\{\delta x_i\}$ into the eigenspace spanned by the eigenvectors of the Laplacian coupling matrix $\mathbf{G} = \mathbf{C} + \mathbf{I}$ (where $\mathbf{I}$ is the identity matrix of the same dimension as $\mathbf{C}$), then the set of equations described by Eq. (2) can be transformed into N decoupled variational equations of the form

$$\delta\dot{\mathbf{y}}_i = [\mathbf{DF}(\mathbf{x}_s) - \varepsilon\lambda_i\mathbf{DH}(\mathbf{x}_s)]\delta\mathbf{y}_i, \tag{3}$$

where $0 = \lambda_1 < \lambda_2 < \cdots < \lambda_N$ are the eigenvalues of $\mathbf{G}$, and $\delta\mathbf{y}_i$ is the ith mode of the perturbations. Let Λ_i be the largest Lyapunov exponent calculated from Eq. (3) for the ith mode; then the stability of this mode is determined by the sign of Λ_i: The model is stable if $\Lambda_i \leqslant 0$ and is unstable if $\Lambda_i > 0$. The first mode (associated with λ_1) represents the motion parallel to the synchronous manifold, i.e., the trajectory of a single oscillator, which is always unstable due to the chaotic nature of the isolated-node dynamics.

Network symmetry, as well as partial synchronization, sets in when dividing the eigenvalues (modes) into groups. For a given topological symmetry, $\mathbf{S}$, of the network structure, we can always construct its corresponding permutation matrix, $\mathbf{R}_{N\times N}$, as follows. If the exchange of the pair of nodes i and j in the network (according to the topological symmetry) does not change the network structure, we set $r_{ij} = r_{ji} = 1$; otherwise, we set $r_{ij} = r_{ji} = 0$. For the permutation matrix, we have $\mathbf{R}\mathbf{R}^{-1} = \mathbf{R}^2 = \mathbf{I}$, with $\mathbf{I}_{N\times N}$ the identity matrix. Let $\mathbf{M}$ be the transformation matrix of $\mathbf{R}$, i.e., $\mathbf{M}^{-1}\mathbf{R}\mathbf{M} = \mathbf{R}'$ (with $\mathbf{R}'$ the diagonal matrix); then the Laplacian coupling matrix can be transformed into the blocked form

$$\mathbf{G}' = \mathbf{M}^{-1}\mathbf{G}\mathbf{M} = \begin{pmatrix} \mathbf{B} & 0 \\ 0 & \mathbf{D} \end{pmatrix}, \tag{4}$$

where $\mathbf{B}$ and $\mathbf{D}$ are, respectively, n_1 and n_2 dimensional submatrices, with $n_1 + n_2 = N$. Because $\mathbf{G}'$ and $\mathbf{G}$ are similar matrices, they have the same set of eigenvalues. However, for the blocked matrix $\mathbf{G}'$, the eigenvalues are divided into two groups: n_1 eigenvalues from $\mathbf{B}$ and n_2 eigenvalues from $\mathbf{D}$. It is just the distribution of the two groups of eigenvalues that governs the stability of the partial synchronization state, as shown in the following.

It is worth noting that by the transformation matrix, $\mathbf{M}$, the state vector, $\mathbf{X} = [\mathbf{x}_1, \ldots, \mathbf{x}_N]^T$, is transformed into the form $\mathbf{Y} = [\mathbf{y}_1, \ldots, \mathbf{y}_{n1}, \mathbf{y}'_1, \ldots, \mathbf{y}'_{n2}]^T$, where $\mathbf{y}_m = \mathbf{x}_i - \mathbf{x}_j$ and $\mathbf{y}'_m = \mathbf{x}_i + \mathbf{x}_j$ $(m = 1,2,\ldots,n_1)$ are, respectively, the state difference and summation of the paired nodes, (i,j), under the symmetry $\mathbf{S}$. Therefore, by the transformation of Eq. (4) the phase space is actually separated into two orthogonal subspaces: one is spanned by the eigenvectors of $\mathbf{B}$, which characterizes the synchronization error of the paired nodes, i.e., $\mathbf{Y}^{tr} = [\mathbf{y}_1, \ldots, \mathbf{y}_{n1}]^T$; the other one is spanned by the eigenvectors of $\mathbf{D}$, which characterizes the manifold of partial synchronization, i.e., $\mathbf{Y}^{\mathrm{syn}} = [\mathbf{y}'_1, \ldots, \mathbf{y}'_{n2}]^T$. This technique of phase space separation is essentially the same as those employed in previous studies of partial synchronization [16–22].

As the manifold of partial synchronization is embedded in the n_2 dimensional subspace spanned by the eigenvectors of $\mathbf{D}$, we know from the function of the transformation matrix that the null eigenvalue $\lambda_1 = 0$ is contained in this submatrix. Here we reorder the eigenvalues of $\mathbf{D}$ as $0 = \lambda_1^{\mathrm{syn}} < \lambda_2^{\mathrm{syn}} \leqslant \cdots \leqslant \lambda_{n2}^{\mathrm{syn}}$ and call the spanned subspace the *synchronous subspace*. In a similar way, we reorder the eigenvalues of $\mathbf{B}$ as $\lambda_1^{tr} \leqslant \lambda_2^{tr} \leqslant \cdots \leqslant \lambda_{n1}^{tr}$. Since the subspace spanned by the eigenvectors of $\mathbf{B}$ characterizes the perturbations transverse to the synchronous manifold for partial synchronization, we thus give it the name *transverse subspace*. To make the partial synchronization state stable, it is necessary that all the transverse modes of the perturbations are damping with time. More specifically, we should have $\Lambda(\varepsilon\lambda_l^{tr}) < 0$ for $l = 1,\ldots,n_1$. Meanwhile, to avoid the trivial state of global synchronization, it is also necessary that as least one of the nontrivial modes in the synchronous subspace remains unstable; i.e., $\Lambda(\varepsilon\lambda^{\mathrm{syn}}) > 0$ for some mode (modes) of $\mathbf{D}$. These are the two necessary conditions for having a stable partial synchronization state. (Exceptions may arise when the oscillators are globally coupled, or when there are periodic windows in the synchronization transition. These exceptional cases are discussed in Sec. V.)

By the above eigenvalue method, we now give an analysis on the stability of the state $\mathbf{P}_{S1} = (a,b,c,d,c,b)$ shown in Fig. 1(d). First, from the reflection symmetry, $\mathbf{S}_1$, we can

construct the permutation matrix, which reads

$$\mathbf{R} = \begin{pmatrix} 1 & 0 & 0 & 0 & 0 & 0 \\ 0 & 0 & 0 & 0 & 0 & 1 \\ 0 & 0 & 0 & 0 & 1 & 0 \\ 0 & 0 & 0 & 1 & 0 & 0 \\ 0 & 0 & 1 & 0 & 0 & 0 \\ 0 & 1 & 0 & 0 & 0 & 0 \end{pmatrix}. \quad (5)$$

Second, by calculating the eigenvectors of **R**, we can construct the following transform matrix:

$$\mathbf{M} = \begin{pmatrix} 0 & 0 & 1 & 0 & 0 & 0 \\ 0 & 1/\sqrt{2} & 0 & 0 & 1/\sqrt{2} & 0 \\ -1/\sqrt{2} & 0 & 0 & 0 & 0 & 1/\sqrt{2} \\ 0 & 0 & 0 & 1 & 0 & 0 \\ 1/\sqrt{2} & 0 & 0 & 0 & 0 & 1/\sqrt{2} \\ 0 & -1/\sqrt{2} & 0 & 0 & 1/\sqrt{2} & 0 \end{pmatrix}. \quad (6)$$

Finally, by the transform matrix **M**, we can transform the coupling matrix, **G**, into the blocked matrix, **G**′, with the two submatrices reading

$$\mathbf{B} = \begin{pmatrix} -4/3 & -1/3 \\ -1/3 & -4/3 \end{pmatrix}, \quad (7)$$

and

$$\mathbf{D} = \begin{pmatrix} -1 & 2/7 & 5/7\sqrt{2} & 0 \\ 2/7 & -1 & 0 & 5/7\sqrt{2} \\ \sqrt{2}/3 & 0 & -2/3 & 1/3 \\ 0 & \sqrt{2}/3 & 1/3 & -2/3 \end{pmatrix}. \quad (8)$$

For the submatrix **B**, we have $(\lambda_1^{tr},\lambda_2^{tr}) = (1,1.67)$; for the submatrix **D**, we have $(\lambda_1^{syn},\lambda_2^{syn},\lambda_3^{syn},\lambda_4^{syn}) = (0,0.63,1.05,1.65)$. Since the null eigenvalue belongs to **D**, according to our definition, the synchronous and transverse subspaces thus are spanned by the eigenvectors of **D** and **B**, respectively.

For the chaotic Lorenz oscillator and the coupling function we have employed, the value of $\Lambda(\varepsilon\lambda)$, as calculated from Eq. (3), is negative only when $\varepsilon\lambda = \sigma > \sigma_c \approx 8.3$ [Fig. 2(a)] [40,41]. For $\varepsilon = 8.4$ [the coupling strength used in Fig. 1(d)], the values of σ for the two transverse modes are $\sigma_1^{tr} = \varepsilon\lambda_1^{tr} = 8.4$ and $\sigma_2^{tr} = \varepsilon\lambda_2^{tr} = 13.9$. As $\sigma_{1,2}^{tr} > \sigma_c$, both transverse modes are stable. The first condition for partial synchronization thus is satisfied. For the synchronous modes, the values of σ are $(\sigma_1^{syn},\sigma_2^{syn},\sigma_3^{syn},\sigma_4^{syn}) = (0,5.23,8.72,13.7)$. Since $\sigma_2^{syn} < \sigma_c$, the second nontrivial mode of the synchronous subspace is unstable. Therefore, the second condition for partial synchronization is also satisfied. To better describe the stabilities of the synchronous and transverse modes, we plot Fig. 2(a). Since $\lambda_1^{tr} > \lambda_2^{syn}$, by the requirements $\Lambda(\varepsilon\lambda_1^{tr}) > 0$ and $\Lambda(\varepsilon\lambda_2^{syn}) < 0$, we can also obtain analytically the region in the parameter space for generating the stable partial synchronization state, which is $\varepsilon \in (\varepsilon_1', 13.1)$, with $\varepsilon_1' = \sigma_c/\lambda_2^{syn}$ the critical coupling strength for partial synchronization predicted by the method of eigenvalue analysis. This prediction is in a good agreement with the numerical results shown in Fig.1.

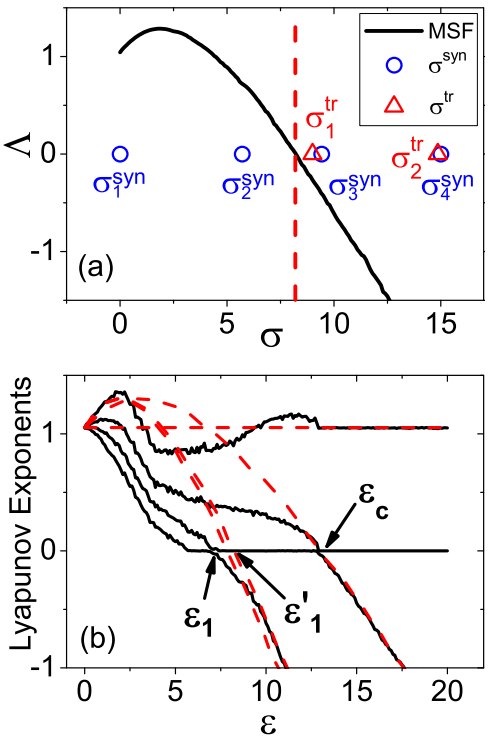

FIG. 2. (Color online) (a) With $\varepsilon = 9.0$, the eigenvalue analysis of the stability of the partial synchronization state $\mathbf{P}_{S1} = (a,b,c,d,c,b)$. The MSF curve ($\Lambda$) is calculated according to Eq. (3), where $\Lambda(\sigma)$ is negative when $\sigma = \varepsilon\lambda > \sigma_c \approx 8.3$. The modes in the transverse and synchronous subspaces are denoted by triangles and circles, respectively, where λ^{syn} is calculated from the submatrix **D** and λ^{syn} is calculated from the submatrix **B**. (b) The variations of the four largest Lyapunov exponents as a function of the coupling strength. The solid lines are obtained by direct simulations, and the dashed lines are derived from the MSF curve. The slight difference of the critical coupling strengths for partial synchronization is due to the simplified reference manifold adopted in the method of eigenvalue analysis.

The above method of eigenvalue analysis explains also why the other two symmetries of the network, $\mathbf{S}_2$ and $\mathbf{S}_3$, do not give rise to stable partial synchronization states. For the reflection symmetry $\mathbf{S}_2$, we have $(\lambda_1^{tr},\lambda_2^{tr},\lambda_3^{tr}) = (0.63,1.65,1.67)$ and $(\lambda_1^{syn},\lambda_2^{syn},\lambda_3^{syn}) = (0,1,1.05)$. As $\lambda_1^{tr} < \lambda_2^{syn}$, when the two transverse modes are in the stable regime (i.e., satisfying the first condition), all the nontrivial synchronous modes are already in the stable regime, which breaks the the second condition. As such, although it is potentially supported by the symmetry $\mathbf{S}_2$, the pattern $\mathbf{P}_{S2} = (a,b,b,a,c,c)$ cannot be observed in the synchronization transition. This is also the case for the rotation symmetry $\mathbf{S}_3$. The rotation symmetry is supportive to the pattern $P_{S3} = (a,b,c,a,b,c)$, but, because $\lambda_1^{tr} < \lambda_2^{syn}$, this pattern is also not observable in the process of synchronization transition.

It is noticed that, although in good agreement, the critical coupling strength predicted by the method of eigenvalue analysis is slightly different from that of numerical simulations. More specifically, from the numerical results we have $\varepsilon_1 \approx 8.1$ [Fig. 1(c)], while the eigenvalue analysis gives $\varepsilon_1' \approx 8.3$. That is, the system reaches the partial synchronization state at a

smaller coupling strength than predicted. This discrepancy could be attributed to the simplified reference manifold we have adopted in the stability analysis. In the partial synchronization state, the synchronous manifold is embedded in the synchronous subspace, which is of the dimension $3 \times n_2$. In general, the stability analysis of the partial synchronization state should refer to a manifold with the similar dimension. However, for the sake of simplicity, in our method of eigenvalue analysis we have used the global synchronization manifold as the reference, which is three dimensional and is actually unstable in the synchronous subspace. To suppress this instability, a larger coupling strength therefore is needed, i.e., $\varepsilon_1' > \varepsilon_1$. This reasoning is supported by the numerical simulations of Lyapunov exponents. In Fig. 2(b), we plot two sets of Lyapunov exponents obtained by different approaches, one by direct simulation and the other one derived from the MSF curve. In the MSF approach, the Lyapunov exponents are just $\Lambda(\sigma_i)$ for the modes, which can be readily read from the MSF curve. It is seen that for the global synchronization transition, the two approaches give the same critical coupling strength (the point where the second largest Lyapunov exponent crosses 0), but for the partial synchronization transition, there is a small difference between the two critical coupling strengths (the point where the second largest Lyapunov exponent crosses 0).

IV. TRANSITION BETWEEN DIFFERENT PARTIAL SYNCHRONIZATION STATES

What happens to the synchronization transition if the network has more than one stable partial synchronization state? To check this out, we adjust slightly the network of Fig. 1(a) by increasing $w_{1,4}$ to 3. Like the original network, the modified network also possess three topological symmetries, $\mathbf{S}_{1,2,3}$, which are supportive to three different synchronous patterns. By the method of eigenvalue analysis presented in Sec. III, the stabilities of the patterns can be well analyzed, with the details as follows. For the reflection symmetry $\mathbf{S}_1$, the eigenvalues for the synchronous and transverse submatrices are $(\lambda_1^{\rm syn},\lambda_2^{\rm syn},\lambda_3^{\rm syn},\lambda_4^{\rm syn}) = (0,0.73,0.83,1.77)$ and $(\lambda_1^{tr},\lambda_2^{tr}) = (1,1.67)$, respectively. As $\lambda_1^{tr} > \lambda_{2,3}^{\rm syn}$, the synchronous pattern $\mathbf{P}_{S1} = (a,b,c,d,c,b)$ supported by $\mathbf{S}_1$ is stable when $\varepsilon > \varepsilon_1 = \sigma_c/\lambda_1^{tr} \approx 8.3$. For the reflection symmetry $\mathbf{S}_2$, the eigenvalues for the synchronous and transverse submatrices are $(\lambda_1^{\rm syn},\lambda_2^{\rm syn},\lambda_3^{\rm syn}) = (0,0.73,1.77)$ and $(\lambda_1^{tr},\lambda_2^{tr},\lambda_3^{tr}) = (0.83,1,1.67)$, respectively. We have $\lambda_1^{tr} = 0.83 > \lambda_2^{\rm syn} = 0.73$. As such, the synchronous pattern $\mathbf{P}_{S2} = (a,b,b,a,c,c)$ supported by $\mathbf{S}_2$ will be also stable if $\varepsilon > \varepsilon_2 = \sigma_c/\lambda_1^{tr} = 10.12$. As the rotation symmetry $\mathbf{S}_3$ is a combination of $\mathbf{S}_1$ and $\mathbf{S}_2$, i.e., $\mathbf{S}_3 = \mathbf{S}_1 \otimes \mathbf{S}_2$, the system actually presents the pattern $\mathbf{P}_{S3} = (a,b,b,a,b,b)$ when $\varepsilon > \varepsilon_2$. In the meantime, by the method of eigenvalue analysis, we can also obtain the critical coupling strength for global synchronization, $\varepsilon_c = \sigma_c/\lambda_2^{\rm syn} \approx 11.3$. The eigenvalue analysis therefore predicts the following: For $\varepsilon \in (\varepsilon_1,\varepsilon_2)$, only the pattern $\mathbf{P}_{S1} = (a,b,c,d,c,b)$ is stable; for $\varepsilon \in [\varepsilon_2,\varepsilon_c]$, two stable patterns, $\mathbf{P}_{S1}$ and $\mathbf{P}_{S2} = (a,b,b,a,c,c)$, coexist and the system presents the pattern $\mathbf{P}_{S3} = (a,b,b,a,b,b)$; for $\varepsilon > \varepsilon_c$, the system reaches the global synchronization.

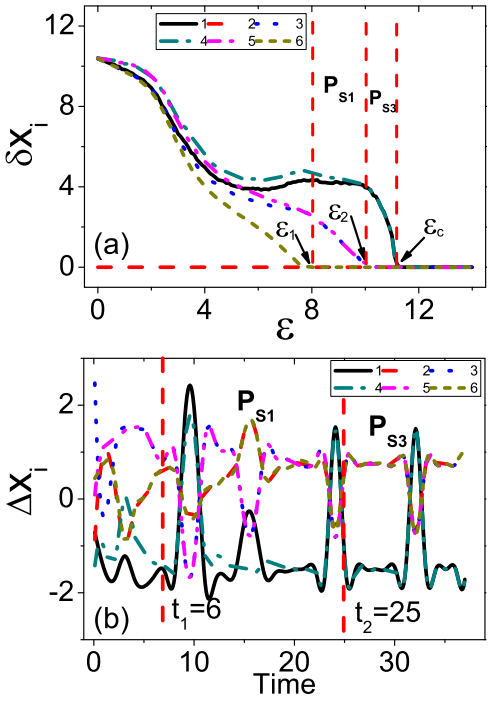

FIG. 3. (Color online) The network structure is the same as Fig. 1(a), but with $w_{1,4} = 3$. (a) The variation of the synchronization relationship of the oscillators, as described by the synchronization error $\delta x_i = \langle |x_i - x_2| \rangle$, as a function of the coupling strength. The patterns $\mathbf{P}_{S1} = (a,b,c,d,c,b)$ and $\mathbf{P}_{S3} = (a,b,b,a,b,b)$ appear at ε_1 and ε_2, respectively. (b) With $\varepsilon = 10.8$, the time evolution of the normalized synchronization errors, $\Delta x_i = (x_i - \bar{x})/\Delta x_{\rm ave}$. The pattern $\mathbf{P}_{S1}$ is realized in an earlier time than the pattern $\mathbf{P}_{S3}$.

The above predications are well verified by numerical simulations. In Fig. 3(a), we plot the variation of the synchronization relationship among the oscillators as a function of the coupling strength. It is seen that, as the coupling strength increases, the oscillators are first synchronized to the pattern $\mathbf{P}_{S1} = (a,b,c,d,c,b)$ (at about $\varepsilon = 8.1 \approx \varepsilon_1$), then to the pattern $\mathbf{P}_{S3} = (a,b,b,a,b,b)$ (at about $\varepsilon = 10.1 \approx \varepsilon_2$), and finally to the state of global synchronization (at about $\varepsilon = 11.3 \approx \varepsilon_c$). To get more details on the generation of the pattern $\mathbf{P}_{S3}$, we take $\varepsilon = 10.8$ and plot the time evolution of the normalized synchronization errors in Fig. 3(b). Interestingly, it is found that in generating the pattern $\mathbf{P}_{S3}$, the two stable patterns, $\mathbf{P}_{S1}$ and $\mathbf{P}_{S2}$, are realized at different time instants. Specifically, the pattern $\mathbf{P}_{S1}$ is realized at about $t_1 = 6$, while the pattern $\mathbf{P}_{S2}$ is realized at about $t_2 = 25$. The different synchronization times of the patterns can be attributed to their different stabilities, with the following reasoning. For each pattern, the most unstable transverse mode is always associated with the eigenvalue λ_1^{tr} (for the adopted node dynamics), which is about 1 and 0.83 for the patterns $\mathbf{P}_{S1}$ and $\mathbf{P}_{S2}$, respectively. According to the MSF curve shown in Fig. 2(b), when $\varepsilon = 10.8$ [Fig. 3(b)], we have $\Lambda^{S1}(\varepsilon\lambda_1^{tr}) \approx -1.04$ for the pattern $\mathbf{P}_{S1}$, and $\Lambda^{S2}(\varepsilon\lambda_1^{tr}) \approx -0.88$ for the pattern $\mathbf{P}_{S2}$. As $\Lambda^{S1} < \Lambda^{S2}$, the pattern $\mathbf{P}_{S1}$ thus has a higher stability than $\mathbf{P}_{S2}$, resulting in the different synchronization times.

In studying synchronization transition, an important issue is about the system dynamics at the neighborhood of the

critical coupling strengths [9,32]. In previous studies of chaos synchronization in regular networks, a general finding is that, in the neighborhood of ε_c, i.e., the critical coupling strength for global synchronization, the system dynamics undergoes the process of on-off intermittency [46–50]. More specifically, during the process of system evolution, most of the time the trajectories of the oscillators stay close to the synchronous manifold, i.e., the "off" states, while occasionally the trajectories could depart away from the synchronous manifold, resulting in short-period bursts of large synchronization errors, i.e., the "on" states. Regarding the synchronous manifold as an invariant set in the phase space, the phenomenon of on-off intermittency can be analyzed by the chaos theory, where some important features of on-off intermittency have been revealed, e.g., the power-law distribution of the laminar phase [46,48,49].

In addition to the transition to global synchronization, in our case of nonlocally coupled oscillators, there are also transitions from nonsynchronization to partial synchronization state (at the critical coupling strength ε_1) and from one partial synchronization state to another partial synchronization state (at the critical coupling strength ε_2). As we have mentioned earlier, different from global synchronization, in partial synchronization the invariant set in the phase space, i.e., the synchronous manifold, is high-dimensional and hyperchaotic. For instance, the synchronous manifold for the pattern $\mathbf{P}_{S1} = (a,b,c,d,c,b)$ in Fig. 1(d) is 12 dimensional and has two positive Lyapunov exponents [Fig. 2(a)]. As the intermittent process is largely dependent on the dynamics of the invariant set, it is intriguing to see whether the traditional phenomenon of on-off intermittency (as observed in the transition to global synchronization) can still be observed in the transition from nonsynchronization to partial synchronization or between two different partial synchronization states.

To investigate, we adopt the coupling strength $\varepsilon = 10$, which is slightly below the critical coupling strength ε_2, and monitor the evolution of the system dynamics. As under this coupling strength the pattern $\mathbf{P}_{S1}$ is already stably generated [Fig. 3(a)], we therefore focus on only the stability of the pattern $\mathbf{P}_{S2}$. In Fig. 4(a), we plot the time evolution of the synchronization errors for the paired oscillators (according to pattern $\mathbf{P}_{S2}$), $D_{S2} = |x_1 - x_4| + |x_2 - x_3| + |x_5 - x_6|$. For those moments where the system dynamics is staying close to the pattern, we have $D_{S2} \approx 0$; otherwise the value of D_{S2} will be large. The results in Fig. 4(a) show that, during the process of system evolution, most of the time the value of D_{S2} is close to 0 (the "off" state), but occasionally it could grow to larger values (the "on" state). Clearly, similar to the transition to global synchronization, the transition to the pattern $\mathbf{P}_{S2}$ is also accompanied by the phenomenon of on-off intermittency.

To investigate the process of on-off intermittency further, we go on to analyze the probability distribution of the length of the laminar phase. Here, the laminar length, τ, refers to the time interval between two adjacent bursts of $D_{S2} > 5$. For the on-off intermittency observed in global synchronization transition, a distinct feature is that the laminar phase follows a power-law scaling, with the scaling exponent $\gamma = -3/2$ [48]. In the inset plot of Fig. 4(a), we plot the laminar-phase distribution of the on-off intermittency obtained with $\varepsilon = 10$. It is seen that, just like the global synchronization transition, the laminar-phase

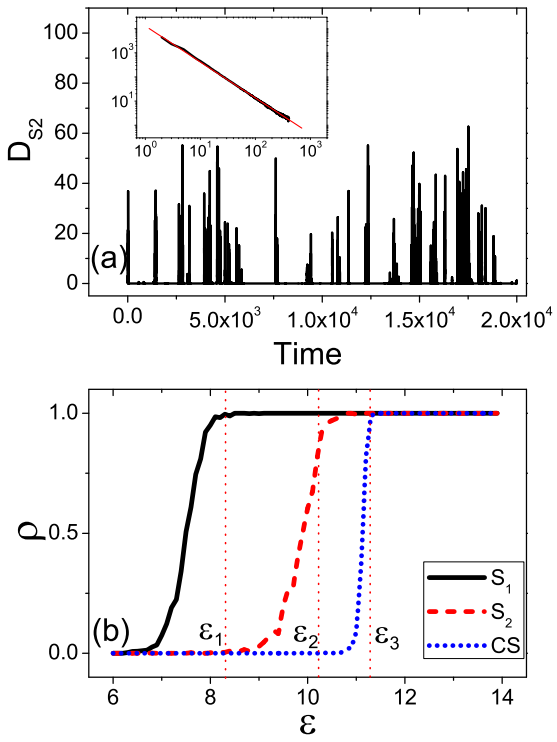

FIG. 4. (Color online) The network is the same as Fig. 3(a) With $\varepsilon = 10$, the process of on-off intermittency. D_{S2} is the pattern synchronization error which measures the closeness of the system dynamics to the partial synchronization state $\mathbf{P}_{S2} = (a,b,b,a,c,c)$. (Inset) The laminar-phase distribution calculated for a time sequence of $T = 1 \times 10^6$, which follows the power-law scaling of the fitted exponent $\gamma \approx -3/2$. (b) The progressive transitions around the critical coupling strengths ε_1, ε_2, and ε_c. ρ is the fraction of time that the system state satisfies $D < 1 \times 10^{-6}$ during the system evolution. Each datum is averaged over 100 realizations.

distribution also follows a power-law scaling, with the fitted exponent $\gamma \approx -3/2$. For on-off intermittency in the transition to global synchronization, another feature typically observed in literature is that, with the increase of the coupling strength, the time intervals of the "off" state will be gradually stretched; i.e., the transition is progressive [47,49,50]. To test whether this feature also exists in the transition to partial synchronization, we vary the coupling strength near ε_2 and check whether the frequency of the system dynamics is close to the pattern $\mathbf{P}_{S2}$. In simulation, for each coupling strength we record 1×10^3 instants of the system evolution (after a transient period of $T = 1 \times 10^3$) and count the number of times it satisfies $D_{S2} < 1 \times 10^{-6}$. The results are plotted in Fig. 4(b). It is seen that, as the coupling strength increases around ε_2, the frequency with which the system stays in the pattern $\mathbf{P}_{S2}$ is gradually increased from 0 to 1. That is, the transition to partial synchronization also proceeds in a progressive fashion.

The above features of on-off intermittency, including the power-law distribution of the laminar phase and the progressive transition in the neighboring region of the critical point, are also observed for the other two transitions, i.e., at ε_1 [the transition from nonsynchronization to the pattern $\mathbf{P}_{S1} = (a,b,c,d,c,b)$] and ε_c [the transition from the pattern $\mathbf{P}_{S3} = (a,b,b,a,b,b)$ to the global synchronization] [Fig. 4(b)].

The numerical results in Fig. 4 thus suggest that, despite the high-dimensional synchronous manifold, the transition behaviors of the partial synchronization states are still governed by the traditional mechanism of on-off intermittency.

V. DISCUSSIONS AND CONCLUSION

Besides the model of networked chaotic Lorenz oscillators, we have also studied other models, including changing the network structure and the node dynamics, where the similar phenomena of synchronization transition have been found. For instance, by a five-node unweighted network [Fig. 5(a)] and adopting the chaotic Rössler oscillator as the node dynamics

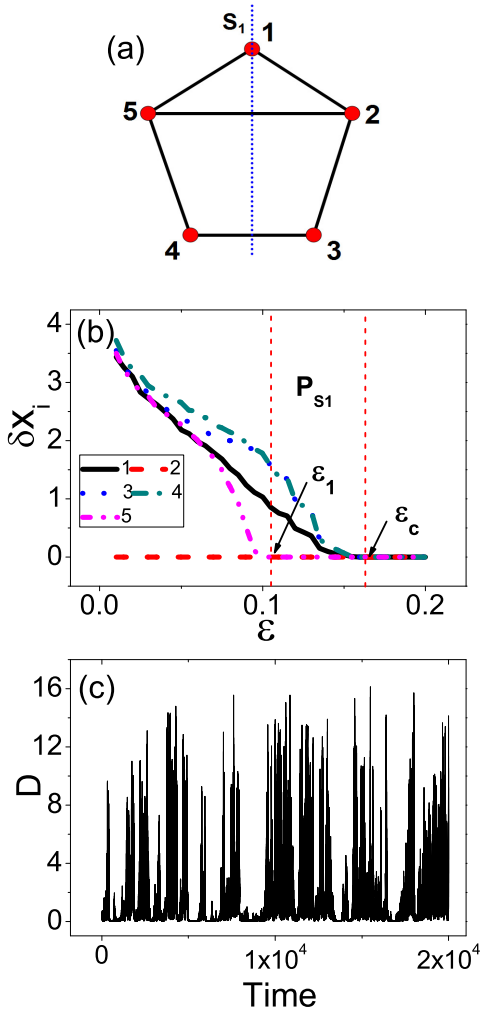

FIG. 5. (Color online) Synchronization transition in networked chaotic Rössler oscillators. The isolated chaotic Rössler oscillator is described by the equations $(dx/dt,dy/dt,dz/dt)^T = [-y-z,x+0.2y,z(x-8.5)+0.2]^T$ [51], and the coupling function is adopted as $\mathbf{H}[\mathbf{x},\mathbf{y},\mathbf{z}]^T = [x,y,0]^T$. (a) The network structure, which possesses the reflection symmetry $\mathbf{S}_1$. (b) The variation of the synchronization relationship of the oscillators, $\delta x_i = \langle |x_i - x_2| \rangle$, as a function of the coupling strength, ε. The system reaches the partial synchronization state (a,b,c,c,b) at $\varepsilon_1 \approx 0.1$ and the global synchronization at $\varepsilon_c = 0.16$. (c) With $\varepsilon = 8.5 \times 10^{-2}$, the intermittent process of the system evolution described by the synchronization error, D, associated with the pattern (a,b,c,c,b).

[51], we have investigated the transition of the system dynamics from nonsynchronization to global synchronization as a function of the coupling strength. In Fig. 5(b), we plot the variation of the synchronization relationship of the oscillators as a function of ε. It is seen that, before the state of global synchronization (at $\varepsilon_c \approx 0.16$), the oscillators reach the partial synchronization state (a,b,c,c,b) (at $\varepsilon_1 \approx 0.1$). Still, the stability of this partial synchronization state, as well as the value of ε_1, can be analyzed by the method of eigenvalue analysis. For the synchronous pattern (a,b,c,c,b) [as supported by the reflection symmetry $\mathbf{S}_1$ indicated in Fig. 5(a)], the eigenvalues of the synchronous and transverse subspaces are, respectively, $(\lambda_1^{\text{syn}},\lambda_2^{\text{syn}},\lambda_3^{\text{syn}}) = (0,0.67,1.5)$ and $(\lambda_1^{tr},\lambda_t r^{tr}) = (1,1.83)$. As $\lambda_1^{tr} > \lambda_2^{\text{syn}}$, the pattern thus is able to be generated. In the meantime, for the Rössler oscillator the critical point of the MSF curve is $\sigma_c = 0.1$ [41]. As such, the pattern is stable when $\varepsilon > \varepsilon_1 = \sigma_c/\lambda_1^{tr} \approx 0.1$. This estimation agrees with the numerical result very well [Fig. 5(b)]. By $\varepsilon = 8.5 \times 10^{-2}$, we plot in Fig. 5(c) the evolution of the synchronization error associated with the pattern (a,b,c,c,b), $D = |x_2 - x_5| + |x_3 - x_4|$, where the phenomenon of on-off intermittency is also presented.

While our studies are based on ideal network models of symmetric topology and identical oscillators, the phenomena we have revealed might be observable in the general networks. In particular, given that the network topology satisfies certain degree of symmetries (not strictly) or that the dynamics of the oscillators are slightly mismatched, the partial synchronization states, although unstable, could be still play important roles in the synchronization transition. For instance, for the network used in Fig. 2 and with $\varepsilon = 9$, the pattern $\mathbf{P}_{S1} = (a,b,c,d,c,b)$ is stable. Now we add a link between nodes 2 and 5 so as to break the reflection symmetry $\mathbf{S}_1$ supporting this pattern. Clearly, with the increase of the weight of the new link, the degree of the reflection symmetry $\mathbf{S}_1$ will gradually deteriorate. However, we find that when the weight of the new link, $w_{2,5}$, is not too large ($w_{2,5} < 0.25$), the system dynamics is still governed by the pattern $\mathbf{P}_{S1}$ [Fig. 6(a)]. A similar phenomenon is also found for the case of nonidentical oscillators. For instance, for the network used in Fig. 2 and with $\varepsilon = 9$, we change gradually the bifurcation parameter, r, of the Lorenz oscillator for node 2 from 35 to 30 and plot the variation of the synchronization relationship of the oscillators. As shown in Fig. 6(b), for a small mismatch of the parameter, $\Delta r < 2$, the paired oscillators (according to the network symmetry $\mathbf{S}_1$) are still well synchronized. It is worthwhile to note that, due to the symmetry of the network topology, in certain circumstances the change of the system parameters has no impact to the stability of the partial synchronization state, e.g., changing the parameter for node 1 or 4 or changing the parameters of the paired nodes (2,6) or (3,6) simultaneously.

The partial synchronization phenomena we have revealed might shed new light on the synchronization behaviors observed in large-scale complex networks. One example is the influence of the network structure on the onset of network synchronization. In network synchronization, a general finding is that, compared to the homogeneous network, the heterogeneous network (of the same network size and connectivity) requires a smaller coupling strength in reaching the onset of synchronization (usually defined as the point

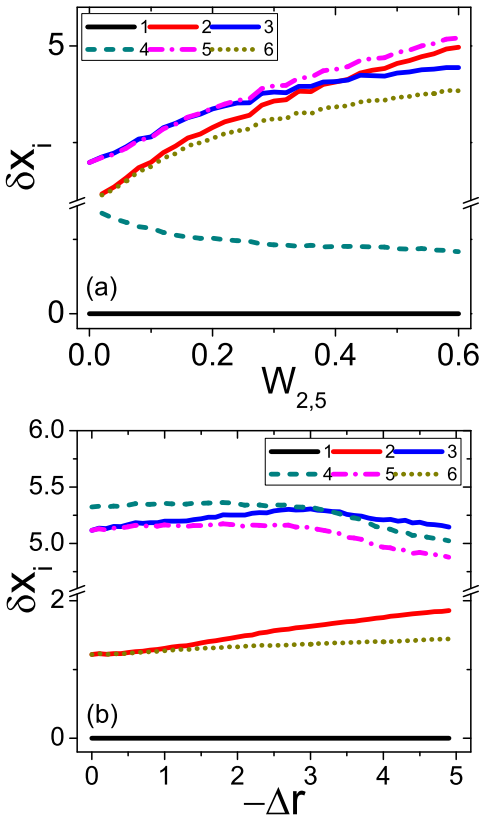

FIG. 6. (Color online) For the network model used in Fig. 2 and with $\varepsilon = 9$, the stability of synchronous pattern $\mathbf{P}_{S1} = (a,b,c,d,c,b)$ under (a) the topological perturbation and (b) the mismatched oscillator parameters. The node synchronization error is defined as $\delta x_i = \langle |x_i - x_1| \rangle$. For the topological perturbation, a new link is added between nodes 2 and 5, with the weight of the new link, $w_{2,5}$, varying from 0 to 0.6. For the parameter mismatch, the system parameter, r, of node 2 varies from 35 to 30.

where the systems order parameter starts to increase from 0) [36]. Previously, this phenomenon has been explained by the property of the extreme eigenvalues of the network coupling matrix, based on the central manifold theory [32]. Our study of partial synchronization might explain this phenomenon from another viewpoint, with the help of a proper characterization of the network symmetry. Unlike the network models employed in the present work, in a large-scale complex network the network topology does not possess any (strict) symmetry, which means that partial synchronization, in principle, cannot be generated. However, as has been discussed in the recent studies, while being short of topological symmetry at the global level, there do exist certain (loosely defined) topological symmetries at the local level for the general complex networks, i.e., a permutation of a few of the network nodes does not affect the network structure [52,53]. With this regard, partial synchronization could still be generated, but in a different manner; e.g., only a few of the network nodes are synchronized.

Comparing to the homogeneous networks (e.g., the random networks), the heterogenous networks (e.g., the scale-free networks) own more local symmetries and thus have a higher propensity for generating partial synchronization of smaller clusters (such as the synchronous motifs), making the onset of synchronization occur at a smaller coupling strength. On the other hand, at the meso- or macroscale, the homogeneous networks present a higher-level symmetry than the heterogenous networks, which is favorable for generating partial synchronization of larger clusters (such as the synchronous communities). This provides an explanation for the sharp synchronization transition of the homogeneous networks under large coupling strength (close to the state of global synchronization) [36]. Therefore, from the viewpoint of partial synchronization, the different paths to synchronization in homogeneous and heterogeneous networks can be simply attributed to their different topological symmetries. It should be pointed out that the above analysis of complex network synchronization is speculative and conjectural, which should be verified carefully by further studies.

A few remarks should be made on the conditions for generating partial synchronization states. First, in studying the partial synchronization, we have employed two typical chaotic models as the local dynamics, namely, the chaotic Lorenz and Rössler oscillators. For these oscillators, during the process of synchronization transition the network dynamics is always chaotic [i.e., with at least one positive Lyapunov exponent, as shown in Fig. 2(b)] and the synchronous manifolds (for both partial or global synchronization) seem to be globally attractive (independent of the initial conditions). However, for other local dynamics, e.g., the chaotic logistic map, the transition process may contain various periodic windows, making the analysis of partial synchronization much more complicated [54]. For instance, in Ref. [11] it has been shown that for globally coupled chaotic logistic maps, global synchronization (of chaotic synchronous manifold) and partial synchronization (of periodic synchronous manifold) could coexist, showing the feature of a riddled basin [13]. Our analysis of partial synchronization cannot be applied to the case of periodic windows. Second, even if a periodic window is avoided in the synchronization transition, the global and partial synchronization may still coexist under certain circumstances. This has been demonstrated in Ref. [18] with three (symmetrically or asymmetrically) coupled chaotic tent maps, where it is shown that in the regime between the riddling and blow-out bifurcations the system may develop to either (strong) partial synchronization or (weak) global synchronization, depending on the initial conditions. In this case, the emergence and stability of global and partial synchronization are two different processes which may occur independently of each other. Apparently, our analysis of partial synchronization cannot be applied to such a case either. Finally, our estimation on the critical coupling strength of partial synchronization is based on the global synchronization manifold, which is a rough approximation of the partial synchronization manifold. When the coupling strength is smaller than ε_c (the critical coupling for global synchronization), a few of the transverse directions (with the number equals the size of synchronous cluster) of the global synchronization manifold will lose their stabilities and span the synchronous subspace [18]. As the coupling strength decreases further, the synchronous subspace will be gradually enlarged and, as a consequence, the partial synchronization manifold will be gradually diverged from the global synchronization manifold. This should be the under-

lying reason for the mismatched critical coupling strength (for generating stable partial synchronization) between the numerical and the theoretical results. The divergence of the partial synchronization manifold from the global synchronization manifold is more evident in the case of multiple partial synchronization; for example, in Fig. 3(a) we have $\varepsilon_1 \approx 8$ numerically for the first bifurcation, while the theoretical analysis gives $\varepsilon_1' \approx 8.3$. Clearly, this mismatch is much larger than that of the second bifurcation at ε_2 (where the mismatch is about 0.1). To improve the theory, an in-depth analysis on the system dynamics near the bifurcation points should be necessary [11–13,17–19].

In summary, from the viewpoint of partial synchronization, we have revisited the problem of synchronization transition in networks of coupled nonlinear oscillators. An interesting finding is that the transition can be clearly divided into different stages, with each stage characterized by a unique state of partial synchronization. With the method of eigenvalue analysis, we have analyzed the stability of the partial synchronization states, in which the crucial dependence of the partial synchronization states on the network symmetries has been revealed. In the neighboring regions of the transition points, we have observed the phenomenon of on-off intermittency, which has the same characterisitcs as that of global synchronization transition. Synchronization transition in networks of asymmetric structure and nonidentical oscillators has been also investigated, and it is found that the partial synchronization states, although unstable, still play important roles in the transition. Our studies shed light on the synchronization transition of networked oscillators and could be a step forward in the exploration of synchronization transition in large-scale complex networks.

ACKNOWLEDGMENTS

The authors thank Professor Z. Zheng for helpful discussions. This work is supported by NSFC under Grant Nos. 11375109 and 11135001 and by the Fundamental Research Funds for the Central Universities under Grant No. GK201303002.

[1] Y. Kuramoto, *Chemical Oscillations, Waves, and Turbulence* (Springer, Berlin, 1984).
[2] A. S. Pikovsky, M. G. Rosenblum, and J. Kurths, *Synchronization: A Universal Concept in Nonlinear Science* (Cambridge University Press, Cambridge, U.K., 2001).
[3] A. Arenas, A. Diaz-Guilera, J. Kurths, Y. Moreno, and C. S. Zhou, Phys. Rep. **469**, 93 (2008).
[4] K. Pyragas, Phys. Rev. E **54**, R4508 (1996).
[5] M. G. Rosenblum, A. S. Pikovsky, and J. Kurths, Phys. Rev. Lett. **78**, 4193 (1997).
[6] C. Zhou and J. Kurths, Phys. Rev. Lett. **88**, 230602 (2002).
[7] Z. Zheng, X. Wang, and M. C. Cross, Phys. Rev. E **65**, 056211 (2002).
[8] D.-S. Lee, Phys. Rev. E **72**, 026208 (2005).
[9] J. Gómez-Gardeñes, S. Gomez, A. Arenas, and Y. Moreno, Phys. Rev. Lett. **106**, 128701 (2011).
[10] M. G. Rosenblum, A. S. Pikovsky, and J. Kurths, Phys. Rev. Lett. **76**, 1804 (1996).
[11] O. Popovych, Yu. Maistrenko, and E. Mosekilde, Phys. Rev. E **64**, 026205 (2001).
[12] A. Pikovsky, O. Popovych, and Yu. Maistrenko, Phys. Rev. Lett. **87**, 044102 (2001).
[13] O. Popovich, Yu. Maistrenko, E. Mosekilde, Phys. Lett. A **302**, 171 (2002).
[14] M. de Sousa Vieira and A. J. Lichtenberg, Phys. Rev. E **56**, R3741 (1997).
[15] D. H. Zanette and A. S. Mikhailov, Phys. Rev. E **57**, 276 (1998).
[16] M. Hasler, Yu. Maistrenko, and O. Popovych, Phys. Rev. E **58**, 6843 (1998).
[17] G. Hu, Y. Zhang, H. A. Cerdeira, and S. Chen, Phys. Rev. Lett. **85**, 3377 (2000).
[18] Yu. Maistrenko, O. Popovych, and M. Hasler, Int. J. Bif. Chaos **10**, 179 (2000).
[19] Y. Zhang, G. Hu, H. A. Cerdeira, S. Chen, T. Braun, and Y. Yao, Phys. Rev. E **63**, 026211 (2001).
[20] L. Huang, K. Park. Y.-C. Lai, L. Yang, and K. Yang, Phys. Rev. Lett. **97**, 164101 (2006).
[21] B. Ao and Z. G. Zheng, Europhys. Lett. **74**, 229 (2006).
[22] T. Dahms, J. Lehnert, and E. Schöll, Phys. Rev. E **86**, 016202 (2012).
[23] C. Fu, Z. Deng, L. Huang, and X. G. Wang, Phys. Rev. E **87**, 032909 (2013).
[24] J. F. Heagy, L. M. Pecora, and T. L. Carroll, Phys. Rev. Lett. **74**, 4185 (1995).
[25] L. M. Pecora, Phys. Rev. E **58**, 347 (1998).
[26] A. L. Barabási and R. Albert, Science **286**, 509 (1999).
[27] D. J. Watts and S. H. Strogatz, Nature (London) **393**, 440 (1998).
[28] X. F. Wang and G. Chen, Int. J. Bifurcation Chaos Appl. Sci. Eng. **12**, 187 (2002).
[29] T. Nishikawa, A. E. Motter, Y.-C. Lai, and F. C. Hoppensteadt, Phys. Rev. Lett. **91**, 014101 (2003).
[30] A. E. Motter, C. S. Zhou, and J. Kurths, Europhys. Lett. **69**, 334 (2005).
[31] X. G. Wang, Y.-C. Lai, and C.-H. Lai, Phys. Rev. E **75**, 056205 (2007).
[32] J. G. Restrepo, E. Ott, and B. R. Hunt, Phys. Rev. E **71**, 036151 (2005).
[33] Z. Zheng, G. Hu, and B. R. Hu, Phys. Rev. Lett. **81**, 5318 (1998).
[34] Y. Wu, J. Xiao, G. Hu, and M. Zhan, Europhys. Lett. **97**, 40005 (2012).
[35] C. S. Zhou and J. Kurths, Chaos **16**, 015104 (2006).
[36] J. Gómez-Gardeñes, Y. Moreno, and A. Arenas, Phys. Rev. Lett. **98**, 034101 (2007).
[37] C. Zhou, L. Zemanová, G. Zamora, C. C. Hilgetag, and J. Kurths, Phys. Rev. Lett. **97**, 238103 (2006).
[38] C. Fu, H. Zhang, M. Zhan, and X. G. Wang, Phys. Rev. E **85**, 066208 (2012).
[39] L. M. Pecora and T. L. Carroll, Phys. Rev. Lett. **80**, 2109 (1998).
[40] G. Hu, J. Z. Yang, and W. Liu, Phys. Rev. E **58**, 4440 (1998).
[41] L. Huang, Q. Chen, Y.-C. Lai, and L. M. Pecora, Phys. Rev. E **80**, 036204 (2009).

[42] X. G. Wang, Eur. Phys. J. B **75**, 285 (2010).
[43] K. Park, Y.-C. Lai, and N. Ye, Phys. Rev. E **70**, 026109 (2004).
[44] E. N. Lorenz, J. Atmos. Sci. **20**, 130 (1963).
[45] A. Pogromsky, G. Santoboni, and H. Nijmeijer, Physica D **172**, 65 (2002).
[46] H. Fujisaka and T. Yamada, Prog. Theor. Phys. **84**, 918 (1985).
[47] E. Ott and J. C. Sommerer, Phys. Lett. A **188**, 39 (1994).
[48] Y. Yu, K. Kwak, and T. Lim, Phys. Lett. A **198**, 34 (1995).
[49] Y. Nagai and Y.-C. Lai, Phys. Rev. E **55**, 1251 (1997).
[50] X. G. Wang, S. Guan, Y.-C. Lai, B. Li, and C. H. Lai, Europhys. Lett. **88**, 28001 (2009).
[51] O. E. Rössler, Phys. Lett. **57A**, 397 (1976).
[52] P. Holme, Phys. Rev. E **74**, 036107 (2006).
[53] Y. Xiao, M. Xiong, W. Wang, and H. Wang, Phys. Rev. E **77**, 066108 (2008).
[54] K. Kaneko, Physica D **41**, 137 (1990).